

Subwavelength microscope that uses frequency scanning for image reconstruction

Stanislav Maslovski

*St. Petersburg State Polytechnical Univ., Radiophysics Dept.,
Polytechnicheskaya 29, 195251, St. Petersburg, Russia**

Pekka Alitalo, and Sergei Tretyakov

Dept. of Radio Science and Engineering, P.O. Box 3000, FI-02015 TKK, Finland[†]

(Dated: November 8, 2018)

A new principle of subwavelength imaging based on frequency scanning is considered. It is shown that it is possible to reconstruct the spatial profile of an external field exciting an array (or coupled arrays) of subwavelength-sized resonant particles with a frequency scan over the whole band of resonating array modes. During the scan it is enough to measure and store the values of the near field at one or at most two points. After the scan the distribution of the near field can be reconstructed with simple post-processing. The proposed near-field microscope has no moving parts.

I. INTRODUCTION

The maximum achievable resolution of any conventional lens, the function of which is based on focusing of electromagnetic radiation, is the wavelength of the used radiation (the limit that is also known as the diffraction limit or the Rayleigh limit). The resolution limit is based on the fact that the evanescent waves, which carry the information about the subwavelength properties of the source, are lost due to their exponential attenuation, and only the propagating waves are restored in the image plane by a focusing lens. The resolution of an imaging device can be greatly improved if this device is able to react to the evanescent part of the spatial spectrum of the incident field. There are several known techniques which allow subwavelength-resolution imaging: superlenses based on the use of materials with negative parameters,^{1,2} superlenses based on phase-conjugation (non-linear three-wave mixing),³ arrays of small resonant particles.⁷⁻¹¹ However, the only mean to actually measure the image-plane near-field distributions at subwavelength scale is the scanning near-field microscope which uses a small moving probe. Recently, hyperlenses which transform evanescent modes into propagating ones have been proposed⁴⁻⁶ with the goal to develop subwavelength microscopes. These devices allow image detection by a stationary system like a charge-coupled device (CCD) matrix, however, the manufacturing technology for hyperlens structures needs further development.

In this paper we introduce a near-field subwavelength imaging device that is based on frequency scanning with following post-processing of measured data. The field is measured only at one or two points in space, and the role of sensor is played by an electrically dense grid of small resonant particles. The device does not use any moving probes, allowing for very fast subwavelength imaging. In this device the conventional measuring of near fields at many points in space is replaced by measuring resonantly enhanced near fields at many frequency points, which allows us to calculate the spatial field distribution. The maximum spatial resolution of the device is limited by

the period of the sensing grid and depends on the quality factor of grid particles as well on the number of particles.

The present method is a development of the approach of our previous paper⁷ which introduced a system of two coupled resonant grids or arrays of small inclusions as a superlens capable for resonant amplification of evanescent fields and creation of images with subwavelength detail. That idea was further extended for enlarging superlenses.⁸ Possible realization in the optical region was also demonstrated.^{9,10} Experimental confirmations in the microwave region were made using grids of small resonant electric dipoles^{7,8} and magnetic dipoles (split rings).¹¹ Grids of resonant particles get strongly excited when the transversal wavenumber k_t of an incident evanescent wave matches the propagation factor of grid's surface wave. We showed both theoretically and experimentally how this effect can be used for resonant amplification of evanescent fields. Because of the resonance, the amplitude of the evanescent wave in the image plane of a dual-grid structure⁷ becomes equal to the amplitude of the evanescent incident wave in the source plane.

Matching of the propagation factors takes place at a certain frequency. The grid of densely packed resonant particles can be modeled by its grid impedance $Z_g(\omega, k_t)$, which connects the surface-averaged tangential electric and magnetic fields.¹² The grid impedance depends on the frequency ω and the propagation factor along the grid plane k_t . The dispersion equation for the surface waves on an impedance grid in free space can be written as

$$Z_g(\omega, k_t) + \frac{Z_0(\omega, k_t)}{2} = 0, \quad (1)$$

where $Z_0(\omega, k_t)$ is the wave impedance of the corresponding free-space plane wave:

$$Z_0(\omega, k_t) = \eta_0 \frac{\sqrt{k_0^2 - k_t^2}}{k_0}, \quad \text{TM modes}, \quad (2)$$

$$Z_0(\omega, k_t) = \eta_0 \frac{k_0}{\sqrt{k_0^2 - k_t^2}}, \quad \text{TE modes}, \quad (3)$$

where $\eta_0 = \sqrt{\frac{\mu_0}{\epsilon_0}}$ and $k_0 = \omega\sqrt{\mu_0\epsilon_0}$. The solutions of

this equation are pairs (ω, k_t) that lie on grid's dispersion curve. If the grid is periodic with the period $d \ll \lambda_0$ (λ_0 is the free-space wavelength), its dispersion curve usually looks like it is shown in Fig. 1(a).

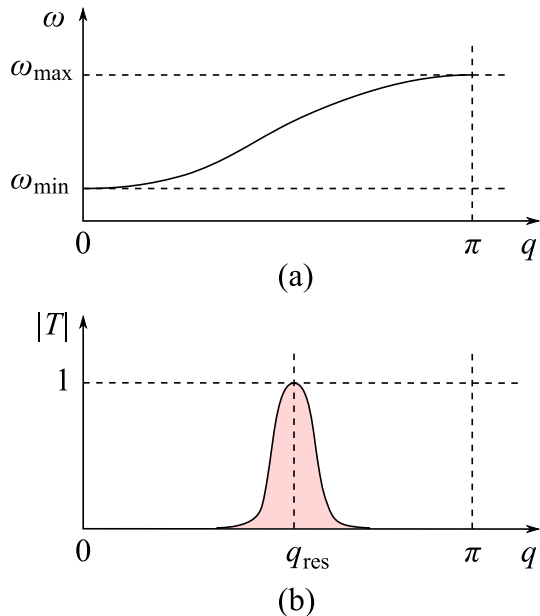


FIG. 1: a) An example dispersion curve of a periodic structure. On the horizontal axis $q = k_t d$. b) Transmission trough a pair of resonating arrays at a given frequency as a function of q .

We see that for an operating frequency $\omega \in [\omega_{\min}, \omega_{\max}]$ there is only a single resonating value for the propagation constant k_t . Scanning the frequency from ω_{\min} up to ω_{\max} we can sequentially excite the surface modes of all possible k_t ranging from 0 to $k_{t\text{max}} = \pi/d$. The amplitude of an excited mode is proportional to the amplitude of the corresponding spectral component of the incident field. Knowing the spatial profile of every surface mode (from the theory or from an initial calibration measurement) we can find the amplitude of the mode from a field measurement done only at a single point in the image plane (or at most at a couple of discrete points, to account for degenerate cases of zero field of certain modes at the measurement point). In a finite-size grid the spectrum of surface modes is discrete. In this case the field measurement is done at discrete frequencies.

It is worth noting that for open structures (in contrast to setups confined inside a closed impenetrable cavity) the surface modes with $0 \leq k_t \leq k_0 \ll \pi/d$ are leaky modes, i.e., they radiate into surrounding space. However, the operation of the microscope is based on the use of eigenmodes with high propagation constants ($k_t \gg k_0$), which are strongly bound to the grid surface and radiate only at inhomogeneities and at the grid ends. Moreover, in some resonant systems such as the metasolens¹³ even the modes with small values of k_t produce a strong resonant response because of a high Q-factor of its resonances (Q is of the order of 10^3).

In a system of two coupled resonant grids⁷ the amplitude of the field in the image plane can be made the same as in the source plane so that the system works as a “perfect lens”¹ at every resonant frequency of the system. This allows us to find the spatial field distribution of the unknown source by weighted integration of measured values, as is explained in Section II. In principle one can use just a single resonating grid. The only difficulty here is that the relation between the amplitude of the excited surface mode and the unknown external field is more complex. The single-grid microscope is explained in Section III.

II. PRINCIPLE OF SPATIAL IMAGING BY FREQUENCY SCANNING

For clarity, let us consider a lens composed of a couple of arrays of small resonating electric dipoles (oriented along the x -axis) placed in between two metal screens: the same system as we used in our measurements.⁷ The dispersion curves of the arrays look like in Fig. 1(a) and the field is measured at the the middle point of the image plane at $x = 0$. To cope with the situation when the x -component of the electric field vanishes at this point for a certain mode it is necessary to have a couple of sensors there: one measures E_x and the other measures the orthogonal component E_z (the longitudinal component). We will also assume that the arrays consist of many particles, so that the spectrum of its modes is practically continuous. An example geometry of the structure is shown in Fig. 2.

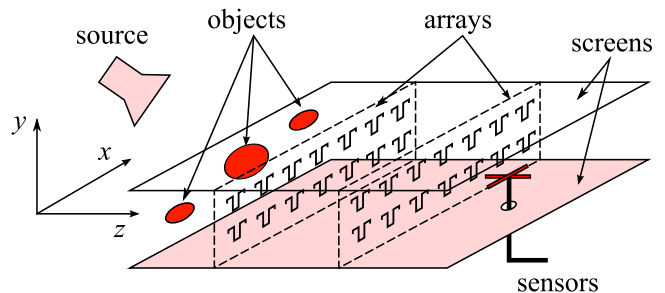


FIG. 2: The side view of a possible lens structure. Two arrays of small particles are positioned along the x -axis. The screening box is open at one of its sides (at the source plane).

Let us assume that the object under study is located in the source plane and it can be excited at the frequencies in the range $[\omega_{\min}, \omega_{\max}]$ and that the properties of the source itself do not change much when we scan the frequency in this range. Practically this means that we have to provide as narrow frequency band of the dispersion curve as possible. In terms of the design of the grids this leads to the known conditions:⁷ the particles must be weakly interacting and be high-Q resonators themselves. At microwave frequencies, electrically small copper-wire meanders are good enough with enough narrow resonant

band.⁷ In the optical range plasmonic metal spheres can be used.^{9,10}

If the source is passive (for example, it is a collection of small pieces of metal) it can be excited with an antenna that illuminates it with a plane wave of the necessary frequency. Because the structures we deal with are most effectively excited with evanescent waves, the illuminating source will not influence the operation of the device (or at least its influence is predictable and can be taken into account in the post-processing stage). It can be a good engineering task to figure out the optimal disposition of the illuminating source and the arrays. In the particular example considered here (Fig. 2), it is assumed that the source electric field is polarized along x and traveling modes are not supported inside the screening box.

For a given frequency $\omega \in [\omega_{\min}, \omega_{\max}]$ the transmission coefficient through the lens as a function of k_x will look like in Fig. 1(b). The characteristic width of the spike is physically determined by the characteristic size L (the array length) of the lens: $\Delta k_x \approx \pi/L$. In principle the spike can be made as narrow as required. The field sensor will measure a kind of average amplitude of the modes with $k_{x\text{res}} - \Delta k_x/2 < |k_x| < k_{x\text{res}} + \Delta k_x/2$.

The device operates as follows. We scan the frequencies from ω_{\min} up to ω_{\max} and store the measured electric field complex amplitudes at every frequency. In the post-processing we use the known spatial profiles of the modes to restore the actual field distribution from the measured field values at the source plane. This is possible via simple integration, because the amplitudes of the fields of every mode are the same at the image and source planes (neglecting dissipation in the grids).⁷ Denoting for even modes: $A^{\text{even}} = E_x^{\text{probe}}$, and for odd modes: $A^{\text{odd}} = -(k_z(\omega)/k_x(\omega))E_z^{\text{probe}}$, the field distribution in the source plane can be expressed as a sum of all modes:

$$E_x(x) = \frac{L}{\pi} \int_{\omega_{\min}}^{\omega_{\max}} \left[A^{\text{even}}(\omega) \cos(k_x(\omega)x) + A^{\text{odd}}(\omega) \sin(k_x(\omega)x) \right] \frac{dk_x(\omega)}{d\omega} d\omega. \quad (4)$$

The coefficient L/π accounts for the spectral density of modes.

As it was said above, in a finite-size grid the spectrum of surface modes is discrete. In this case the field measurement is better to be done at discrete frequencies. We will consider such a system in the next section.

III. SINGLE ARRAY OF RESONANT PARTICLES AS A NEAR-FIELD SENSOR

Let us consider a linear array of resonating particles, Fig. 3. The particles are electrically small passive inclusions that we model by electric dipoles with known polarizabilities. We assume that there are N particles in

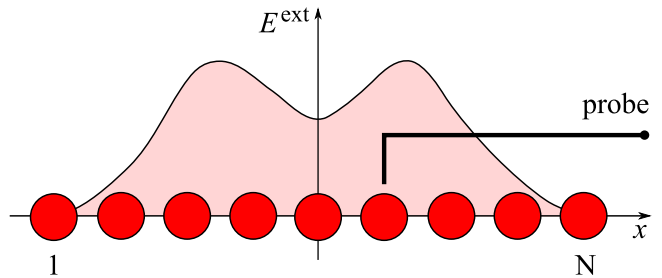


FIG. 3: A linear array of plasmonic nanoparticles as a sub-wavelength microscope sensor. The line shows the electric-field profile to be determined by the microscope. The probe is stationary.

the array and that the array period is d . The electric dipole moments p_k of the array particles can be found from the following system of linear equations:

$$\alpha^{-1}(\omega) p_k - \sum_{n=1, n \neq k}^N \beta_{n-k}(\omega) p_n = E_k^{\text{ext}}, \quad (5)$$

where E_k^{ext} is the external electric field at the position of the particle number k , $\alpha(\omega)$ is the dipole polarizability, and $\beta_{n-k}(\omega)$ accounts for interaction in a pair of dipoles with indices n and k . Our goal is to find the spatial distribution of the external field (that is, find vector E_k^{ext}) from measured field at one point but at several frequencies.

For dipoles orthogonal to the line of the array

$$\beta_m(\omega) = \frac{1}{4\pi\epsilon_0} \left[\frac{k_0^2}{|m|d} - \frac{jk_0}{|m|^2d^2} - \frac{1}{|m|^3d^3} \right] e^{-jk_0|m|d}. \quad (6)$$

For dipoles parallel to the line of the array

$$\beta_m(\omega) = \frac{1}{2\pi\epsilon_0} \left[\frac{jk_0}{|m|^2d^2} + \frac{1}{|m|^3d^3} \right] e^{-jk_0|m|d}. \quad (7)$$

The polarizability of a small resonant dipole can be approximated as

$$\frac{1}{\alpha(\omega)} = \frac{1}{\alpha_0} \left[\frac{\omega_0^2 - \omega^2}{\omega_0^2} + \frac{j\omega}{\omega_0 Q} \right] + \frac{j\eta_0\omega^3}{6\pi c^2}, \quad (8)$$

where α_0 is the static polarizability, ω_0 is the resonant frequency, Q is the quality factor of the particle and the last term accounts for the radiation loss.¹²

The system of equations (5) can be written in matrix form

$$\overline{\overline{A}}(\omega) \cdot \overline{p}(\omega) = \overline{E}^{\text{ext}}, \quad (9)$$

where $\overline{\overline{A}}(\omega)$ is the system matrix, the elements of which can be calculated from the above formulas; $\overline{p}(\omega)$ and $\overline{E}^{\text{ext}}$ are vectors of length N . The eigenmodes of the array can be found from the equation

$$\det \overline{\overline{A}}(\omega) = 0. \quad (10)$$

There are N modes in total. In a system with non-zero loss the modal frequencies defined in this manner are complex quantities with the imaginary part representing the decay of oscillations. In our problem, however, the frequency is defined by the applied external field and is real. Therefore, the array resonances are found as the solutions of equation

$$\text{Re}\{\det \overline{\overline{A}}(\omega_k)\} = 0, \quad (11)$$

where all ω_k are real. Note that the matrix $\overline{\overline{A}}(\omega)$ is almost singular at the frequencies defined by (11). Therefore, its inverse can be approximated as

$$\overline{\overline{A}}^{-1}(\omega_k) \approx \lambda^{-1}(\omega_k) \overline{\overline{P}}(\omega_k), \quad (12)$$

where $\lambda(\omega_k)$ is the eigenvalue of $\overline{\overline{A}}(\omega)$ with the smallest magnitude at $\omega \rightarrow \omega_k$ and $\overline{\overline{P}}(\omega_k)$ is the projection operator for the corresponding eigenvector. Hence, the dipole moments at the resonances are

$$\overline{p}(\omega_k) \approx \lambda^{-1}(\omega_k) \overline{\overline{P}}(\omega_k) \cdot \overline{E}^{\text{ext}}. \quad (13)$$

From here we see that at the resonances the array acts effectively as a filter extracting a single spatial harmonic from the external field.

At the resonances the induced dipole moments are maximal and so is the electric field at the probes that we place near the array. Therefore, it makes sense to measure these fields at resonances. At these frequencies ω_k the field at the location of a probe can be found as

$$E(\omega_k) = \sum_{n=1}^N c_n(\omega_k) p_n(\omega_k), \quad (14)$$

where $c_n(\omega_k)$ are the coefficients describing coupling of the probe to each dipole in the array.

We can rewrite (14) in matrix form

$$E(\omega_k) = \overline{c}^T(\omega_k) \cdot \overline{p}(\omega_k) = \overline{c}^T(\omega_k) \cdot \overline{\overline{A}}^{-1}(\omega_k) \cdot \overline{E}^{\text{ext}}, \quad (15)$$

or, for all N frequencies at once

$$\begin{pmatrix} E(\omega_1) \\ \dots \\ E(\omega_n) \end{pmatrix} = \begin{pmatrix} \overline{c}^T(\omega_1) \cdot \overline{\overline{A}}^{-1}(\omega_1) \\ \dots \\ \overline{c}^T(\omega_n) \cdot \overline{\overline{A}}^{-1}(\omega_n) \end{pmatrix} \cdot \begin{pmatrix} E_1^{\text{ext}} \\ \dots \\ E_N^{\text{ext}} \end{pmatrix}, \quad (16)$$

where the rows in the central matrix are products of \overline{c}^T and $\overline{\overline{A}}^{-1}$ at all the resonant frequencies. Let us recall that we assume that the distribution of the external field does not change when we scan the frequencies in the range $[\omega_1, \omega_N]$.

Finally we can solve (16) for the distribution of the external field:

$$\begin{pmatrix} E_1^{\text{ext}} \\ \dots \\ E_N^{\text{ext}} \end{pmatrix} = \begin{pmatrix} \overline{c}^T(\omega_1) \cdot \overline{\overline{A}}^{-1}(\omega_1) \\ \dots \\ \overline{c}^T(\omega_n) \cdot \overline{\overline{A}}^{-1}(\omega_n) \end{pmatrix}^{-1} \cdot \begin{pmatrix} E(\omega_1) \\ \dots \\ E(\omega_n) \end{pmatrix}. \quad (17)$$

For this solution to exist the matrix in (16) must be non-singular. This can be achieved either by placing a probe at a non-symmetric location with respect to the dipole array or by using more than one probe and intermixing their responses in (16).

IV. NUMERICAL EXAMPLE

As an example let us calculate the response of a linear array of orthogonal dipoles and then restore the distribution of the external field using the method introduced above. We choose the following parameters for the dipole array: the period is such that $k_0 d = 0.1$ at the dipole resonance, the number of dipoles in the array $N = 21$, the quality factor of the particle itself (without radiation loss which is accounted for separately) is $Q = 10^3$, the static dipole polarizability is such that $\alpha_0/(\varepsilon_0 d^3) = 0.5$. This value of the polarizability is rather high. For a metal sphere it corresponds to the radius of $a = d \sqrt[3]{0.5/(4\pi)} \approx 0.34 d$. Note, however, that resonant particles of complex shape or plasmonic particles can provide high values of polarizability even if their size is electrically quite small.

In Fig. 4 the resonant frequencies of the array are plotted as function of their index varying from 1 to 21. These frequencies are found from (11).

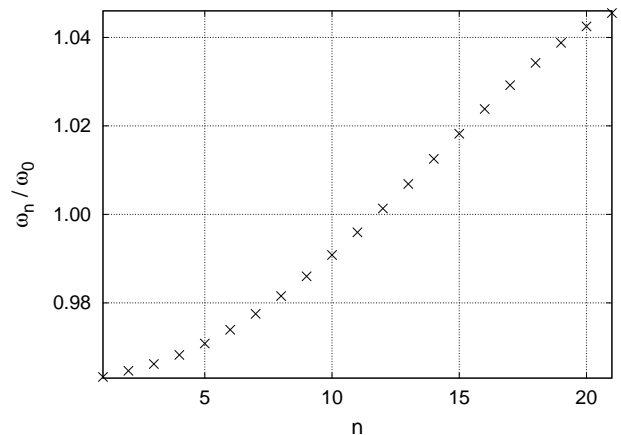


FIG. 4: Resonant frequencies of the dipole array.

The probe is located close to the array at the distance of half a period from the array line. For the probe to be able to react to both symmetric and antisymmetric modes the probe must not be placed in a symmetric position with respect to the array. To find the optimal position we investigate how the condition number of the matrix (16) changes when we move the probe along the array. This is shown in Fig. 5.

The optimal position is found to be in front of the second dipole if counted from the middle of the array. At this point the condition number is about 10. This means that the measurement errors or any other noise

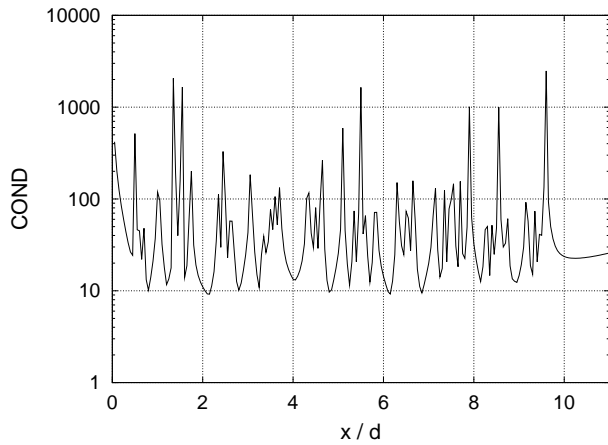


FIG. 5: Condition number of the system matrix as a function of the probe location. Coordinate x is along the array with the origin at the middle dipole.

of relative amplitude of 0.1 will destroy the restoration process. For practical purposes the measurement error must not exceed 10^{-3} – 10^{-2} .

The higher is Q the lower is the condition number. The same holds for the value of α_0 . From the other hand, the condition number grows with increasing the number of dipoles in the array. For an array of about 50 particles to obtain the condition number of 20 one has to provide $Q \sim 10000$ which is hardly achievable. Therefore, with large arrays it would be more practical to employ several probes placed at carefully selected positions.

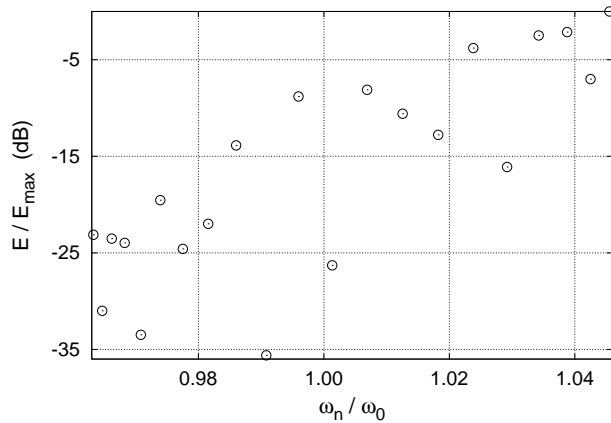


FIG. 6: Electric field amplitude at the location of the probe at different resonant frequencies.

In the following field restoration example we assume the following distribution of the external field:

$$E_k^{\text{ext}} = \frac{1}{1 + (k - 9)^2} + j \frac{1}{1 + (k - 11)^2}. \quad (18)$$

With such an external field in action the amplitude of the electric field at the location of the probe is shown

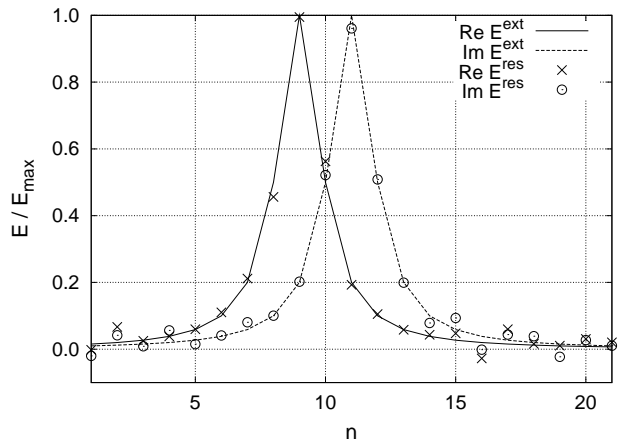


FIG. 7: The profiles of the external field (solid lines) and the restored field (symbols).

in Fig. 6. The probe measures the field only at the array resonant frequencies. In Fig. 7 the restored spatial profile of the external field is compared with the original one given by (18). To show the effect of noise we have added a normally distributed noise of the relative variance of 10^{-2} to the measured probe field. If there is no noise, the restoration is exact, that is, the values of the incident field at the positions of each particle in the array are determined exactly. This means that the microscope resolves spatial details down to the scale of one array period.

V. CONCLUSIONS

In this paper we have presented a near-field imaging principle which allows us to determine spatial distributions of electric or magnetic field with sub-wavelength resolution using observations at several frequencies within a narrow frequency range of sensor's resonances. The field is measured only at one or a few selected points behind the sensing array of resonant particles. The limit for the image resolution is determined by the grid period. We have shown that for reliable measurements it is desirable to use resonant particles with high quality factors and high polarizability values. The evanescent fields emanating from the object under study are effectively enhanced due to resonant excitation of the sensor particles. The necessary range of the frequency scan is reduced if the array particles are weakly coupled to each other. Since the device has no moving parts and there are known means to change the frequency of the probing electromagnetic wave very quickly, this method offers a possibility to make observations of complex sub-wavelength objects very fast and in a non-invasive way. For microwave applications, the sensor can be formed by electrically small metal particles, e.g., in form of a meander⁷ or as dense pack-

ages of split rings (metasolenoids).¹³ For optical applications, the sensor can be potentially realized as grids of plasmonic nanoparticles.^{9,10} Another possibility is to use grids of resonant nanocavities in thin metal layers.¹⁴ The last case has the advantage of reduced coupling be-

tween resonant voids due to field decay in the metal layer. We are now studying dispersion properties of arrays of nanovoids in metal near an interface with free space with some promising results.

* stanislav.maslovski@gmail.com

† sergei.tretyakov@tkk.fi

¹ J. B. Pendry, Phys. Rev. Lett. **85**, 3966 (2000).

² N. Fang, H. Lee, C. Sun, and X. Zhang, Science **308**, 534 (2005).

³ S. Maslovski and S. Tretyakov, J. Appl. Phys. **94**, 4241 (2003).

⁴ Z. Jacob, L. V. Alekseyev, and E. Narimanov, Opt. Express **14**, 8247 (2006).

⁵ I. I. Smolyaninov, Y.-J. Hung, and C. C. Davis, Science **315**, 1699 (2007).

⁶ Z. Liu, H. Lee, Y. Xiong, C. Sun, and X. Zhang, Science **315**, 1686 (2007).

⁷ S. Maslovski, S. Tretyakov, and P. Alitalo, J. Appl. Phys. **96**, 1293 (2004).

⁸ P. Alitalo, S. Maslovski, and S. Tretyakov, Phys. Lett. A

357, 397 (2006).

⁹ P. Alitalo, C. Simovski, A. Viitanen, and S. Tretyakov, Phys. Rev. B **74**, 235425 (2006).

¹⁰ C. Simovski, A. Viitanen, and S. Tretyakov, J. Appl. Phys. **101**, 123102 (2007).

¹¹ M. J. Freire and R. Marques, Appl. Phys. Lett. **86**, 182505 (2005).

¹² S. Tretyakov, *Analytical modeling in Applied Electromagnetics* (Artech House, Boston, 2003).

¹³ L. Jylha, S. Maslovski, and S. Tretyakov, J. Electromagnet. Waves Appl. **19**, 1327 (2005).

¹⁴ S. Coyle, M. C. Netti, J. J. Baumberg, M. A. Ghanem, P. R. Birkin, P. N. Bartlett, and D. M. Whittaker, Phys. Rev. Lett. **87**, 176801 (2001).